

# **Supplementary Material**

**for**

## **Next-generation RNA-Based Fluorescent Biosensors Enable Anaerobic Detection of Cyclic di-GMP**

Xin C. Wang<sup>1</sup>, Stephen C. Wilson<sup>2</sup>, and Ming C. Hammond<sup>1,2</sup>

<sup>1</sup> Department of Molecular & Cell Biology, University of California, Berkeley, 94720; USA

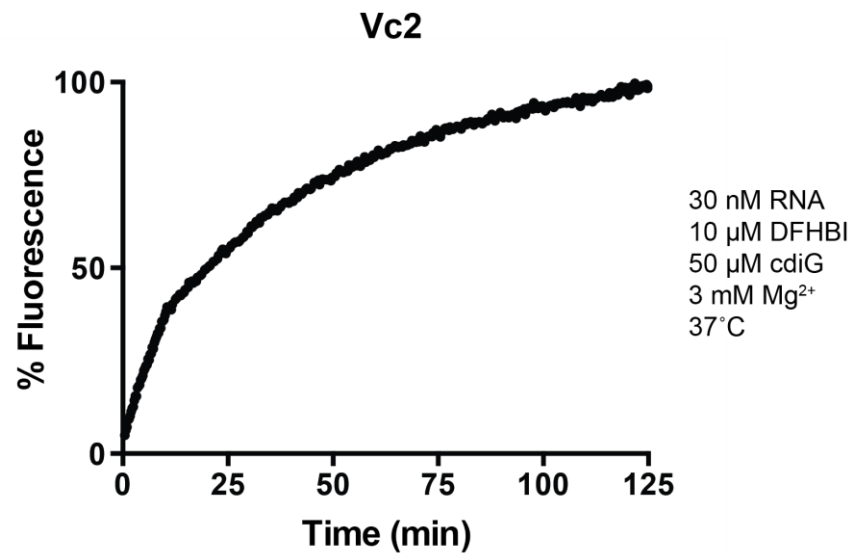
<sup>2</sup> Department of Chemistry, University of California, Berkeley, 94720; USA

**Supplementary Figures 1-12**

**Supplementary Methods**

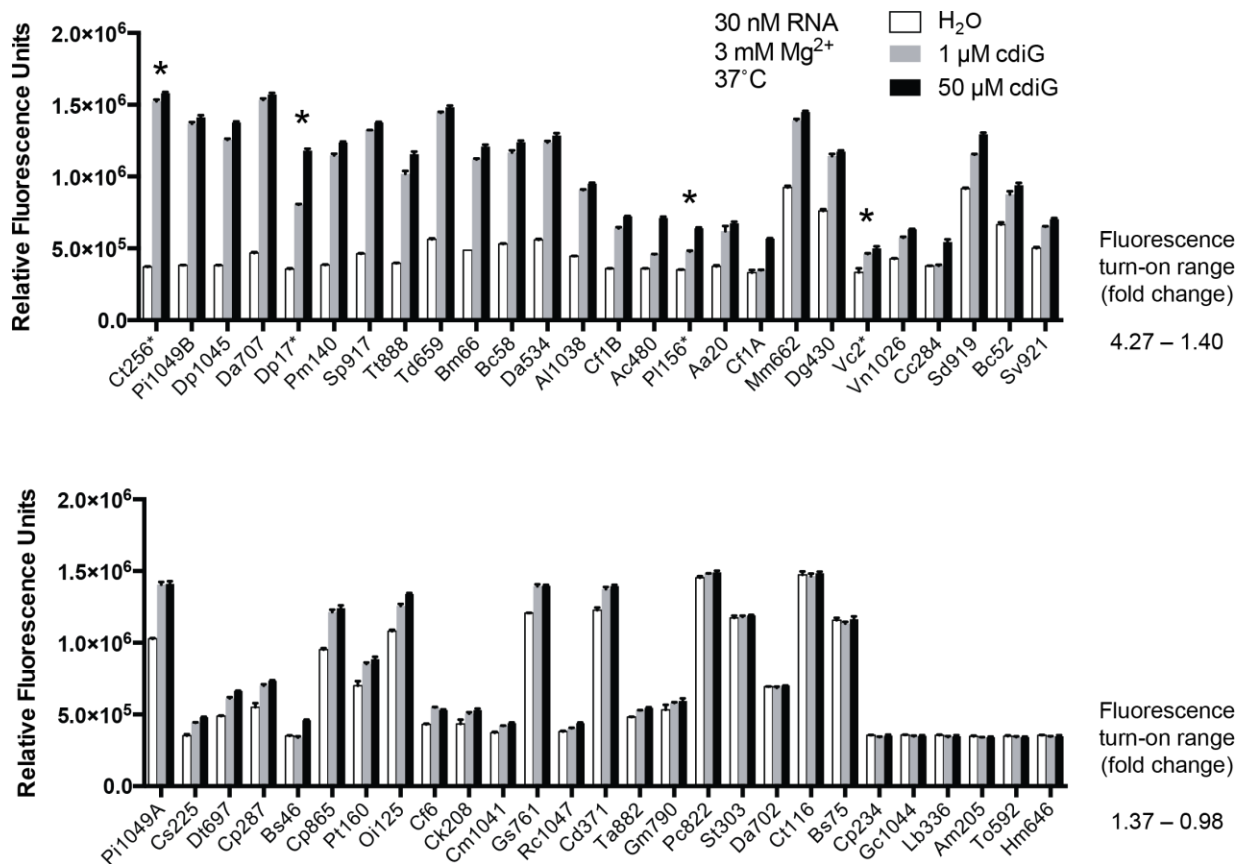
**Supplementary Tables 1-3**

## Supplementary Figures



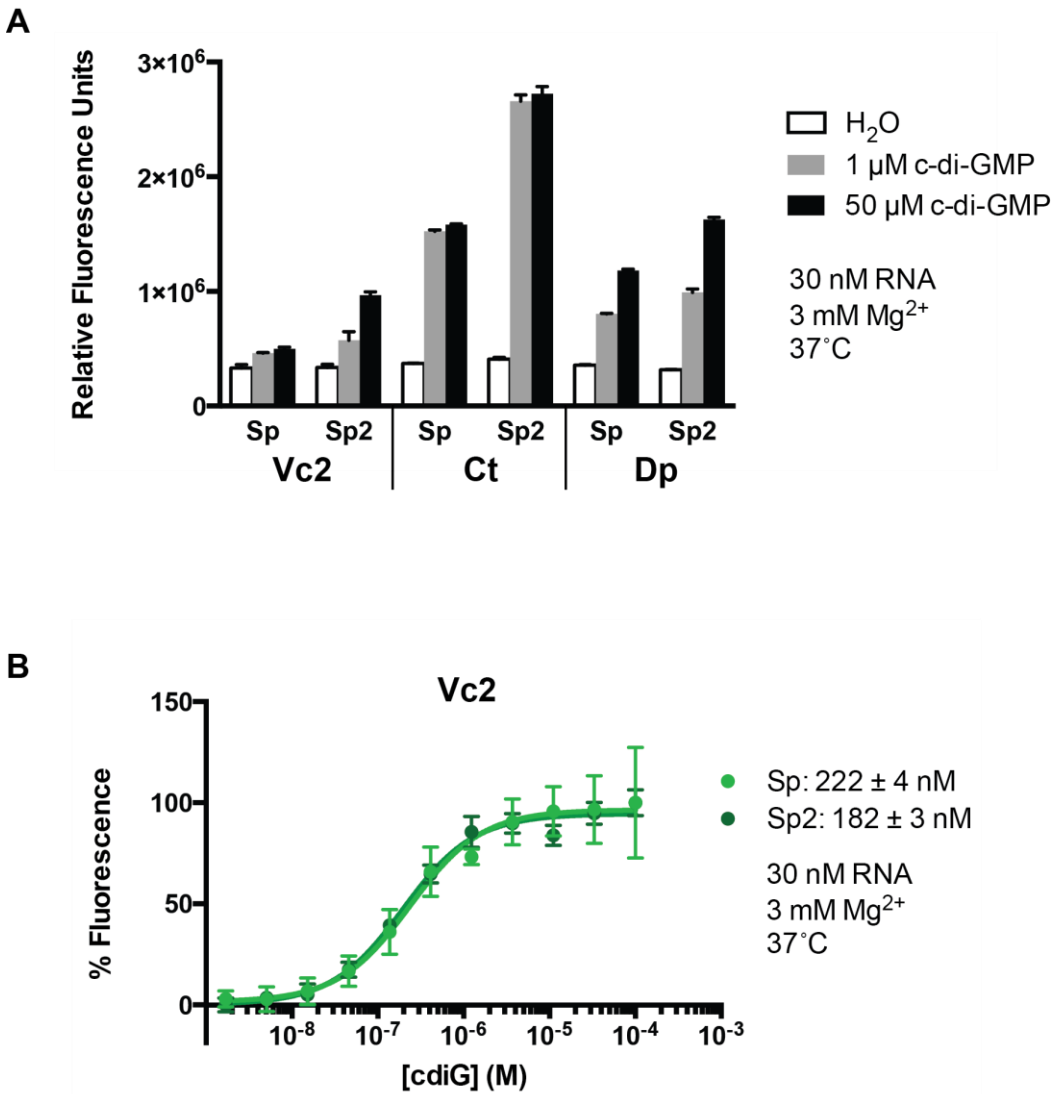
**Supplementary Figure S1.** Vc2 fluorescence turn-on kinetics.

As Fig. 3C, but over a 125-minute time range. Values are an average of three independent experiments.



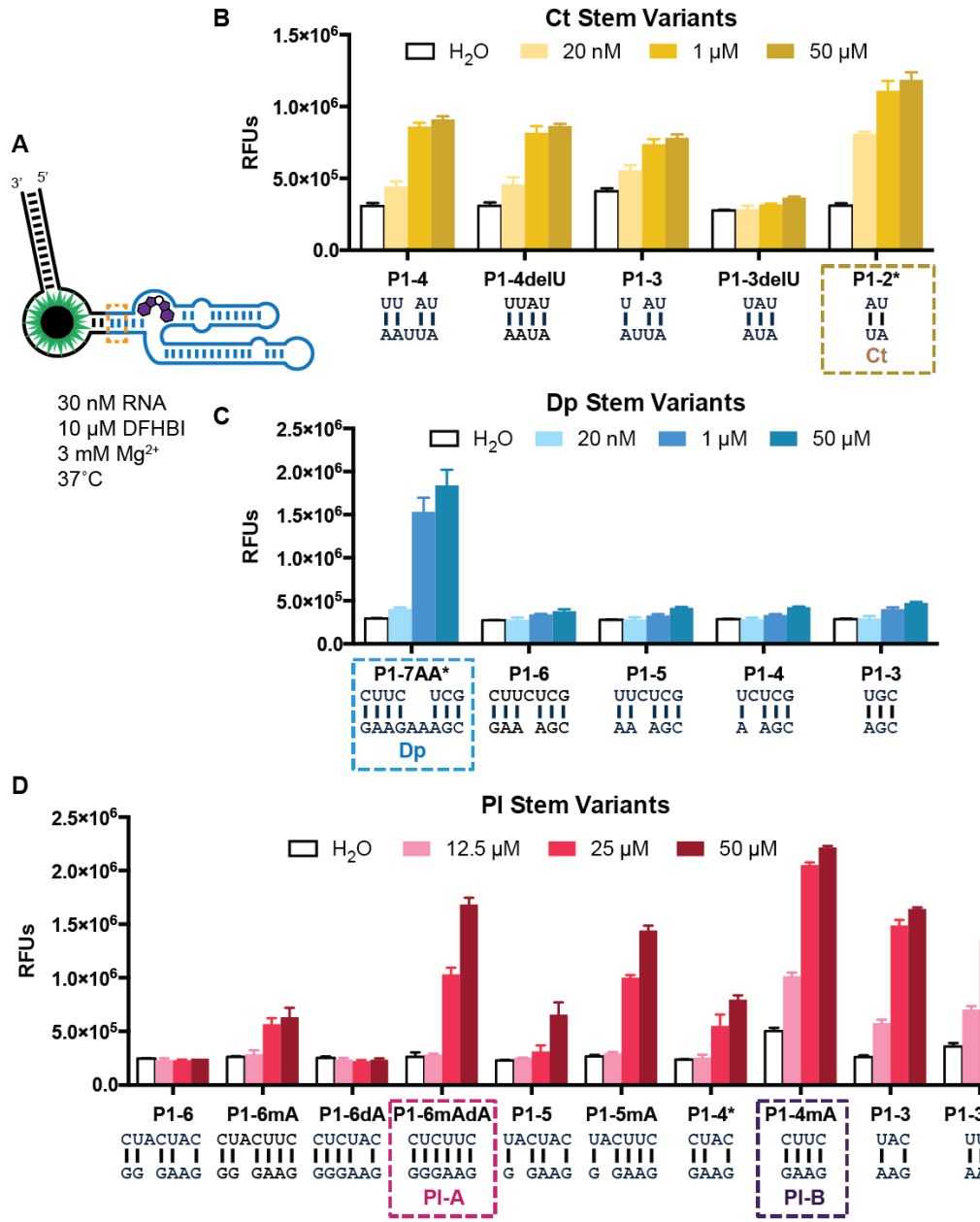
**Supplementary Figure S2.** Phylogenetic screen of GEMM-I riboswitch aptamers fused to Spinach.

A total of 52 GEMM-I-Spinach biosensors were assayed *in vitro* for their relative fluorescence in the presence of 0 ( $\text{H}_2\text{O}$ ), 1, and 50  $\mu\text{M}$  c-di-GMP. The biosensors are displayed from left to right, top to bottom, in order of decreasing fluorescence turn-on, as defined by the relative fluorescence at 50  $\mu\text{M}$  c-di-GMP divided by that at 0  $\mu\text{M}$  c-di-GMP. The asterisks indicate biosensors upon which additional analysis was performed (Ct256, Dp17, PI156), as well as the first-generation sensor Vc2. Error bars represent the standard deviation of three independent experiments with duplicate samples. Also see Figure 2.



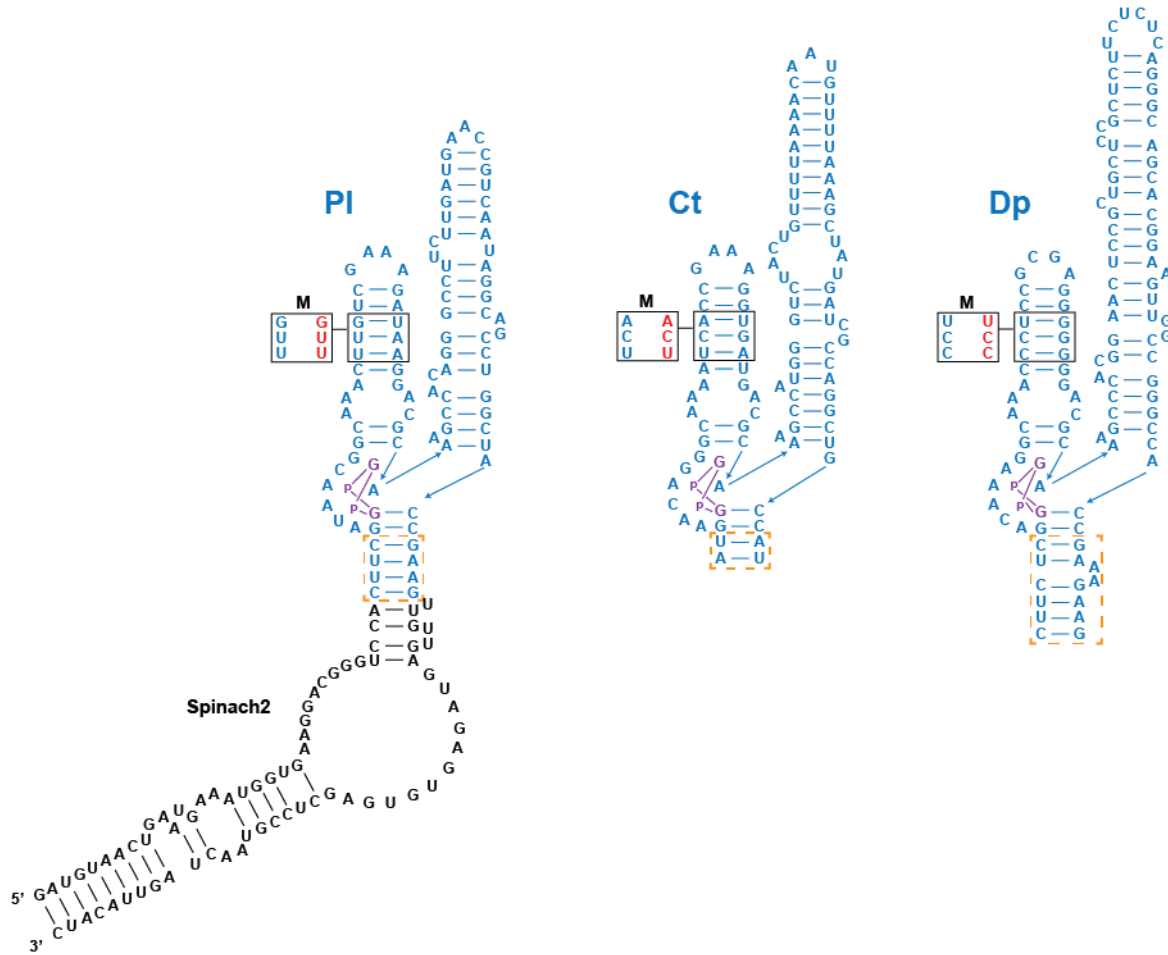
**Supplementary Figure S3.** Spinach vs. Spinach2 biosensors.

- In vitro* fluorescence activation of biosensors with different riboswitch aptamers (Vc2, Ct, and Dp) fused to either Spinach (Sp) or Spinach2 (Sp2), in the presence of 0 ( $\text{H}_2\text{O}$ ), 1, and 50  $\mu\text{M}$  c-di-GMP. Error bars represent the standard deviation of three independent experiments with duplicate samples.
- Ligand (c-di-GMP) affinity of Vc2-Spinach (Sp, light green) vs. Vc2-Spinach2 (Sp2, dark green). Points and error bars represent averages and standard deviations, respectively, from three independent replicates with duplicate samples. Best-fit curves are also shown, and the  $K_D$ s of each biosensor are listed in the legend.



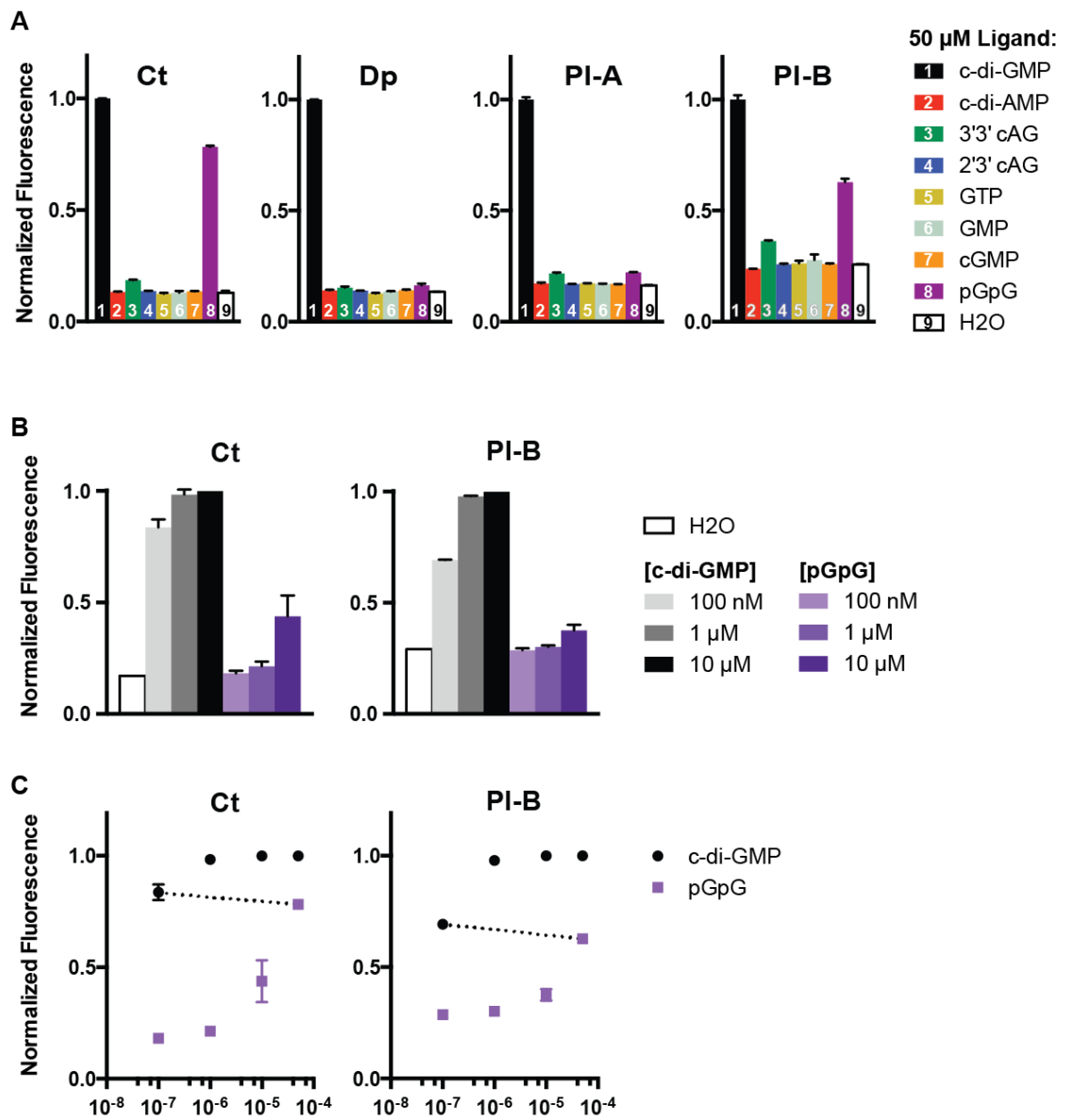
**Supplementary Figure S4.** Transducer stem variants.

- A. Schematic diagram of biosensor, with Spinach2 segment in black, the riboswitch aptamer in blue, and the transducer stem region outlined with an orange dotted rectangle, which corresponds to the stem sequences shown in parts (B)-(D). The experimental conditions for parts (B)-(D) are shown.
- B-D. Fluorescence turn-on of the Ct-Spinach2, Dp-Spinach2, and PI-Spinach2 biosensor stem variants with no or different concentrations of c-di-GMP. The stem sequences are listed with the top strand in the 5' to 3' direction, as if superimposed on the transducer stem region in part (A). The original stem screened in **Supplementary Figure 2** is denoted with an asterisk, while the final second-generation biosensors are boxed. Stems labeled P1-N are wild-type sequences, where N is supposed to correspond to the number of predicted base-pairs.



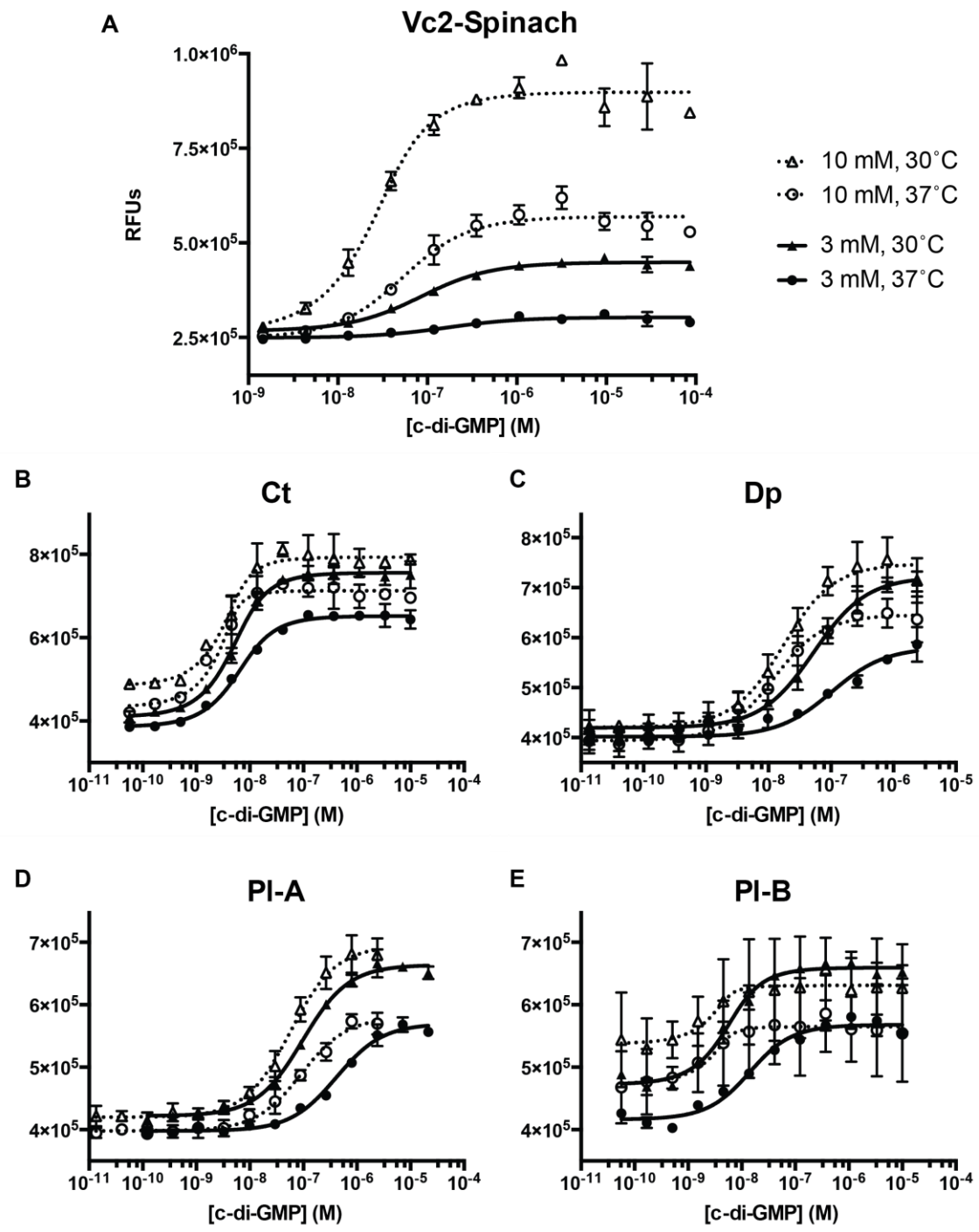
**Supplementary Figure S5.** Secondary structure diagrams.

Sequence and secondary structure of Spinach2-riboswitch fusions. The Spinach2 sequence is in black, the riboswitch aptamer sequence in blue, and the varied transducer stem sequence in the orange box. Depicted sequences are the sequences for second-generation biosensors PI-B, Ct, and Dp. The bound ligand is denoted in purple, and the non-binding mutant (M) sequences are shown. The Ct and Dp sequences are depicted without the Spinach2 aptamer sequence.



**Supplementary Figure S6.** Biosensor ligand selectivity.

- Relative fluorescence of the four second-generation biosensors with 50  $\mu$ M of various ligands: c-di-GMP (1, black), cyclic di-AMP (cdiA, 2, red), 3'-5', 3'-5' cyclic AMP-GMP (3'3' cAG, 3, green), 2'-5', 3'-5' cyclic AMP-GMP (2'3' cAG, 4, blue), GTP (5, yellow), GMP (6, grey), cGMP (7, orange), pGpG (8, purple), and no ligand (9, white). For each biosensor, fluorescence levels were normalized to signal with c-di-GMP.
- Relative fluorescence of Ct (left) and PI-B (right) with 100 nM, 1  $\mu$ M, and 50  $\mu$ M c-di-GMP (light gray, dark gray, and black, respectively) and pGpG (light purple, purple, and dark purple, respectively). For each biosensor, fluorescence levels were normalized to signal with 50  $\mu$ M c-di-GMP.
- Same data as parts **A** and **B**, but with relative fluorescence of c-di-GMP (black circles) and pGpG (purple squares) on the same graph. The dotted lines connect the biosensor fluorescence response to 100 nM c-di-GMP versus 50  $\mu$ M pGpG.

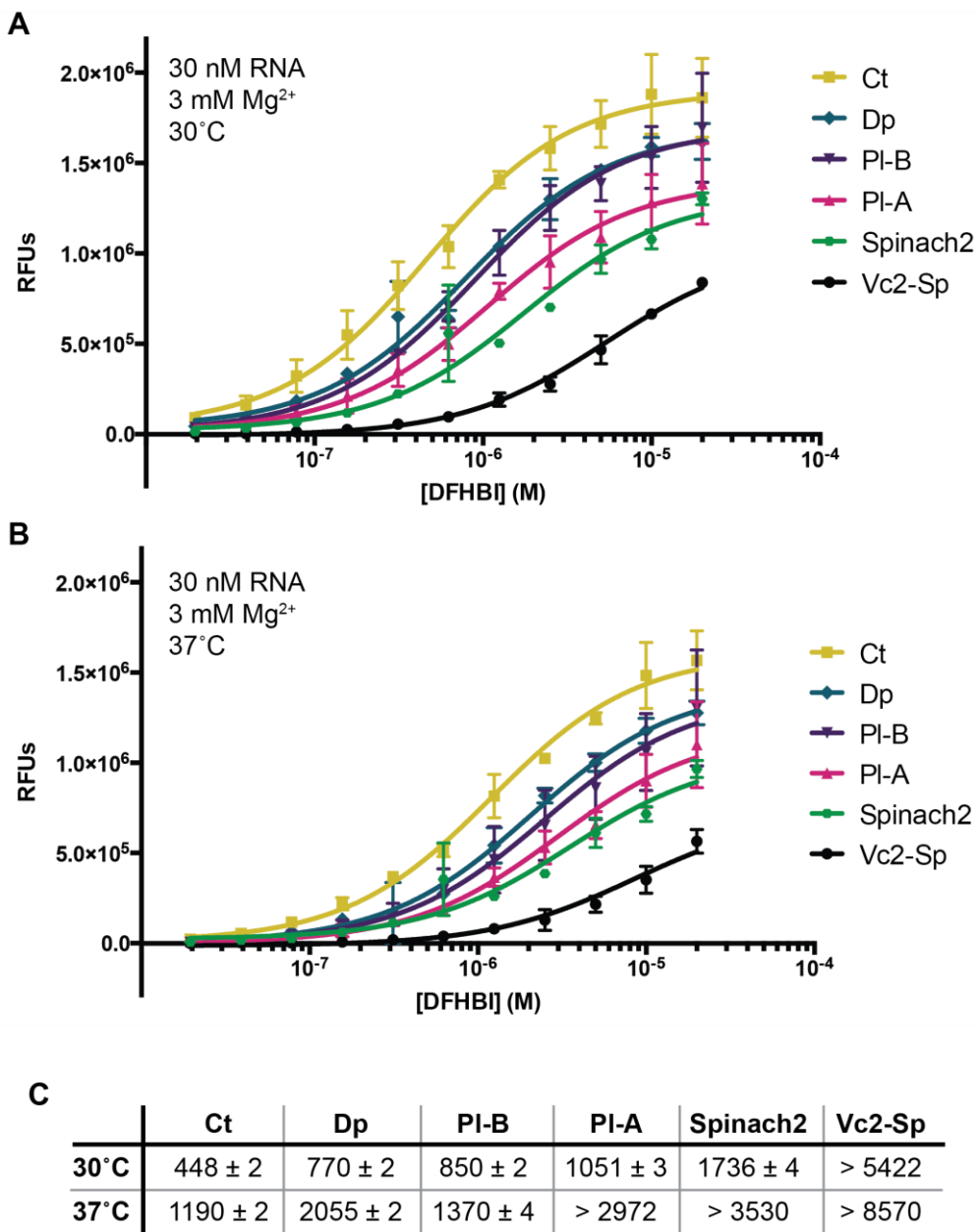


**F**

[Mg <sup>2+</sup> ]	Temp	Vc2	Ct	Dp	PI-A	PI-B
10 mM	30°C	12 ± 2	< 5	15 ± 6	55 ± 10	< 5
	37°C	38 ± 7	< 5	10 ± 27	89 ± 58	< 5
3 mM	30°C	69 ± 2	< 5	50 ± 4	94 ± 8	< 5
	37°C	150 ± 4	< 5	100 ± 3	411 ± 15	12 ± 1

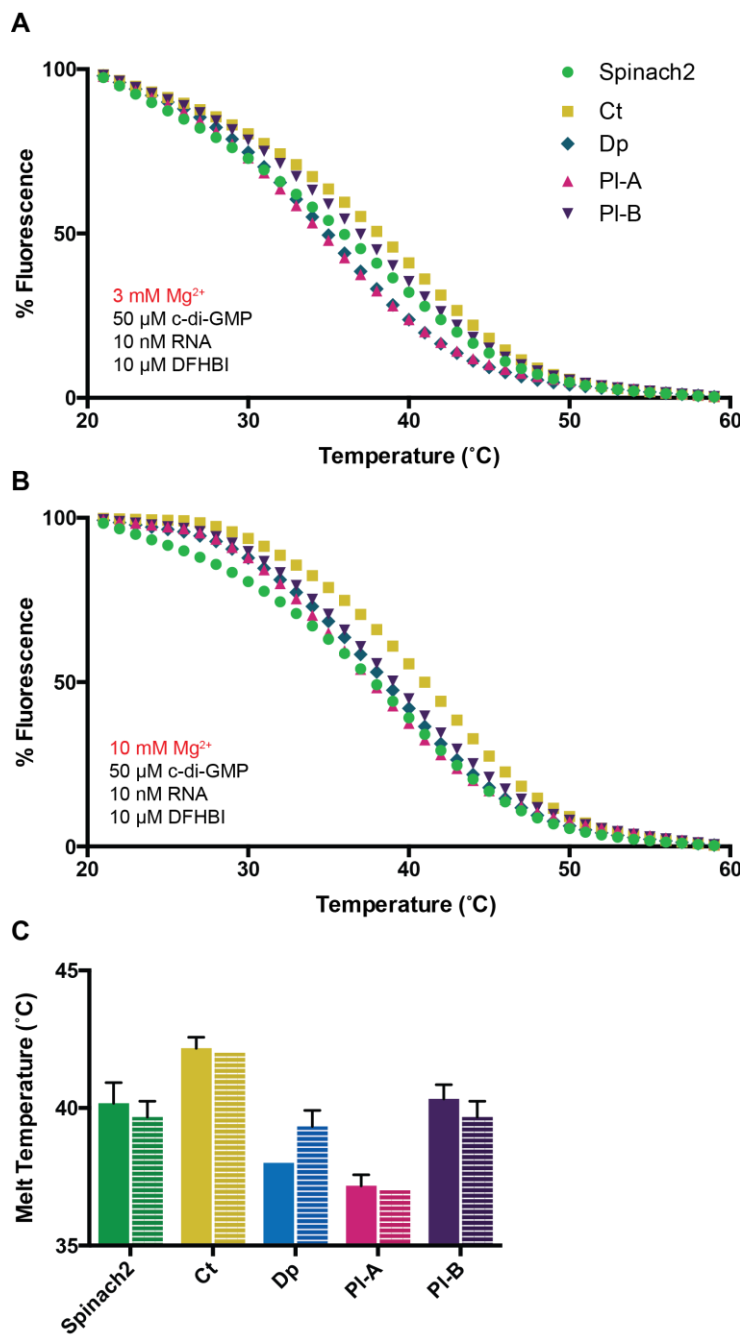
**Supplementary Figure S7.** Biosensor fluorescence with c-di-GMP titration.

Titration of c-di-GMP with the biosensor and DFHBI in varying temperature (30°C – triangles; 37°C – circles) and buffer (3 mM Mg<sup>2+</sup> – filled shapes; 10 mM Mg<sup>2+</sup> – empty shapes) conditions. Each panel displays a separate biosensor (**A.** Vc2; **B.** Ct; **C.** Dp; **D.** PI-A; **E.** PI-B). Points and error bars represent averages and standard deviations of three independent trials; best-fit curves are also shown (3 mM Mg<sup>2+</sup> – solid lines; 10 mM Mg<sup>2+</sup> – dotted lines). All assays included 10 μM DFHBI and 30 nM (Vc2) or 5 nM (Ct, Dp, PI-A, PI-B) RNA. A table of the  $K_D$  values, in nM, are displayed in (**F**).



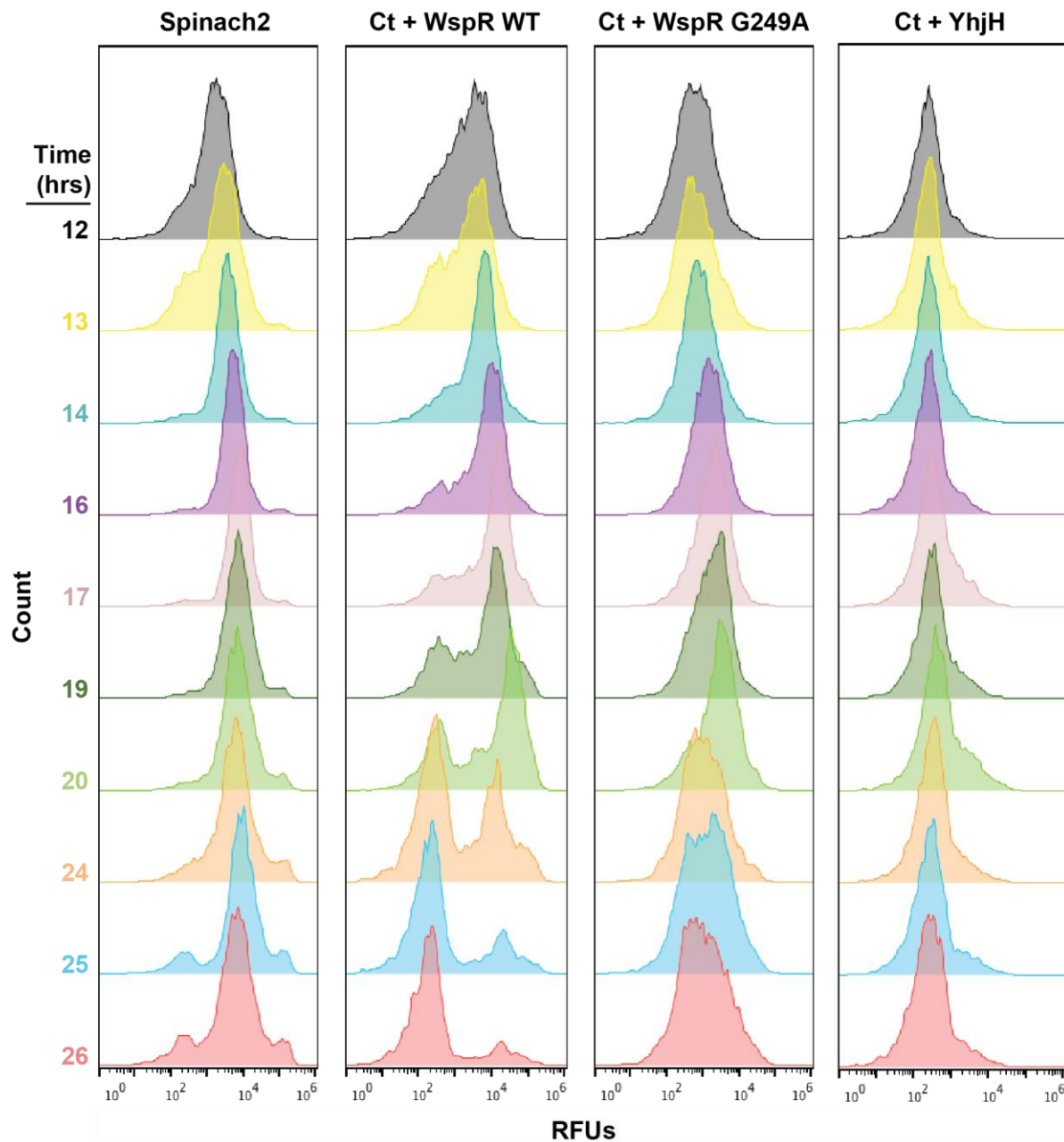
**Supplementary Figure S8.** Biosensor fluorescence with DFHBI titration.

Relative fluorescence of biosensors (Ct: goldenrod squares; Dp: teal diamonds; PI-B: purple downward-pointing triangles; PI-A: pink upward-pointing triangles; Spinach2: green hexagons; Vc2: black circles) with varying concentrations of DFHBI, assessed at **A.** 30°C and **B.** 37°C. Values displayed are background-subtracted, as determined by a no-RNA control sample. Points and error bars represent averages and standard deviations of three independent trials; best-fit curves are also shown. A table of K<sub>D</sub> values of each biosensor for DFHBI, at 30° and 37°C, is displayed in **C.**



**Supplementary Figure S9.** Biosensor fluorescence with temperature ramp.

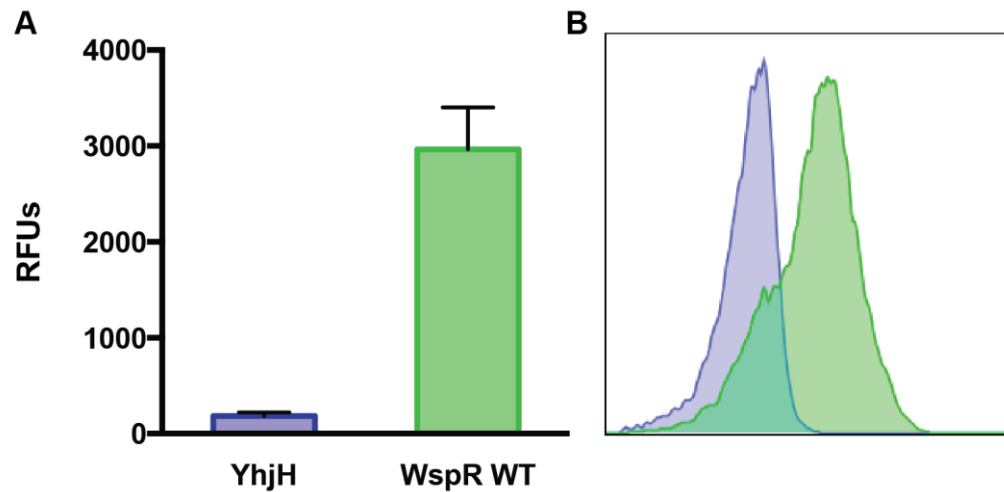
Relative fluorescence of Spinach2 and biosensors (Spinach2: green circles; Ct: goldenrod squares; Dp: teal diamonds; PI-A: pink upward-pointing triangles; PI-B: purple downward-pointing triangles) under saturating conditions of c-di-GMP and DFHBI, assessed over a temperature range between 20-60°C with **A.** 3 mM Mg<sup>2+</sup> and **B.** 10 mM Mg<sup>2+</sup>. Values displayed are normalized and are from one representative trial. The actual melt temperatures, as defined by the inflection point in the melt curve, are graphed in **C.**, with data from 3 mM Mg<sup>2+</sup> (solid bars, left) and 10 mM Mg<sup>2+</sup> (with horizontal lines, right). Values represent averages and standard deviations of three independent trials.



**Supplementary Figure S10. Fluorescence of biosensor-expressing *E. coli* over time.**

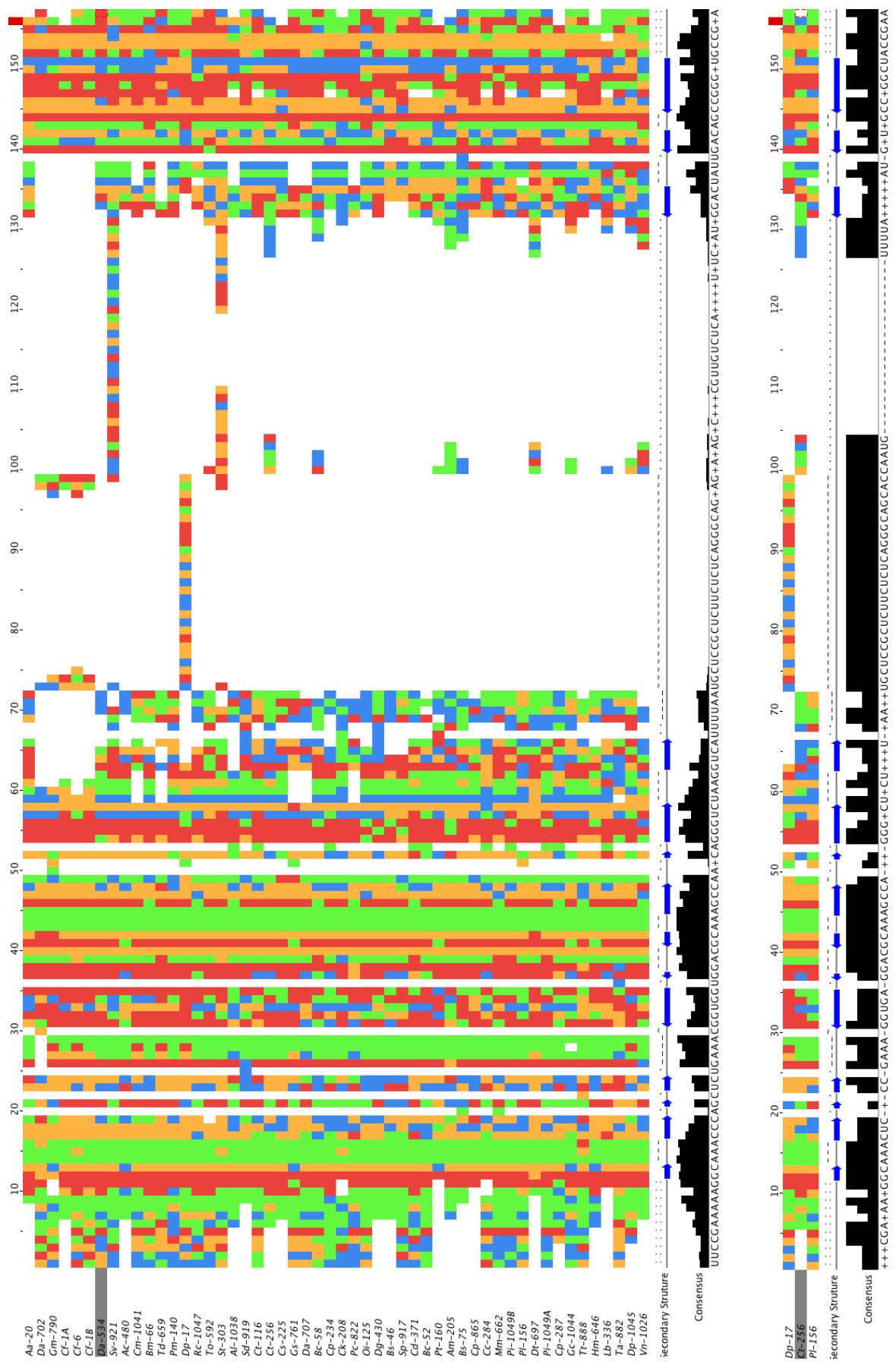
Histograms depicting fluorescence levels of *E. coli* BL21 Star cell populations expressing Spinach2, or Ct biosensor with diguanylate cyclase WspR WT, inactive WspR G249A, or phosphodiesterase YhjH grown aerobically in autoinduction media between 12-26 h. Data shown are 50,000 events from a single representative from three independent replicates.

It should be noted that these cells were grown in autoinduction media as opposed to LB + IPTG in **Figure 4**, so time points cannot be compared between the two figures. In general, we observe increased heterogeneity of biosensor fluorescence at extended incubation times. It seems that 14-16 is optimal for aerobic growth in autoinduction media, but after ~17 h one starts to lose biosensor expression when the biosensor is co-expressed with an enzyme.



**Supplementary Figure S11.** Fluorescence of cells expressing Ct with enzyme off a single plasmid.

- A. Mean fluorescence intensity (MFI) of cells expressing Ct biosensor with YhjH (blue) and WspR WT (green) in BL21 Star cells. Data are from 3 independent replicates ( $n = 30,000$  cells each) represented as mean  $\pm$  SD.
- B. Representative histogram of data from part A.



### **Supplementary Figure S12. Sequence analysis of GEMM-I riboswitches.**

The phylogenetic variants used are presented aligned by secondary structure and colored by nucleotide. Red = A, blue = T, green = C, yellow = G, white = no base. Arrows denoting the secondary structure are shown in blue at the bottom, with opposing arrows indicating paired regions. All 52 sequences are indicated in the upper diagram, while the 3 sequences that were used for the second-generation sensors are isolated in the lower diagram.

Sequences were aligned by secondary structure with Infernal (1) using the GEMM-I covariance model provided in Rfam, accession RF01051 (2). Visualization was performed with JalView (3).

## **Supplementary Methods**

### **Melt curves**

For thermostability measurements, each sample reaction consisted of 100 nM biosensor or Spinach2 RNA, 10 µM DFHBI, and 50 µM c-di-GMP in a buffer containing 40 mM HEPES, 125 mM KCl, and 3 or 10 mM MgCl<sub>2</sub> at pH 7.5. The temperature was then increased from 20°C to 60°C in 1°C increments every 5 minutes, with fluorescence measured at each temperature with the SYBR Green channel of a CFX96 Thermal Cycler (Bio-Rad). Melting temperatures were calculated using the Bio-Rad CFX Manager software (Version 1.5.534.0511) and verified by calculating the inflection point of the first derivative in GraphPad Prism 6 software.

### **Time course**

For fluorescence time course (Supplementary Figure S10), *E. coli* BL21 star cells were transformed with pET31b-Spinach2, or co-transformed with pET31b-Ct-Spinach2 and appropriate enzyme in the pCOLA plasmid. Single colonies were picked and grown at 37 °C in 400 µL of autoinduction media, and 2 µL aliquots were taken at the appropriate time point and diluted in 60 µL of PBS with 50 µM DFHBI-1T. Fluorescence (50,000 events) was analyzed on an Attune NxT flow cytometer (Life Technologies) equipped with a 488 nm laser for excitation and 515/15 filter for emission. Data was analyzed and histograms created on FlowJo (version 10.0.7).

### **Supplementary References**

1. Nawrocki,E.P. and Eddy,S.R. (2013) Infernal 1.1: 100-fold faster RNA homology searches. *Bioinformatics*, **29**, 2933–2935.
2. Griffiths-Jones,S., Bateman,A., Marshall,M., Khanna,A. and Eddy,S.R. (2003) Rfam: an RNA family database. *Nucleic Acids Res.*, **31**, 439–441.
3. Waterhouse,A.M., Procter,J.B., Martin,D.M.A., Clamp,M. and Barton,G.J. (2009) Jalview Version 2--a multiple sequence alignment editor and analysis workbench. *Bioinformatics*, **25**, 1189–1191.

## Supplementary Tables

**Table S1 – Oligos.**

The following oligos were used in this study to generate DNA templates for in vitro transcription (Sp, Sp2), to clone biosensors or fluorescent proteins into pET31b (tSp2, p31b, iLoy, GFP), and to clone yhjH into pETDUET-1. The T7 promoter (in -F) and terminator (in -R) sequences are in red, the tRNA scaffold sequence is underlined, and restriction sites are italicized. All sequences are listed in 5' → 3'.

Sp-F	CCAAGTAATACGACTCACTATAGACCGACTGAATGAAATGGTGAAGG
Sp-R	GACCGCAGTAGTTACGGAGCTCACAC
Sp2-F	CCAAGTAATACGACTCACTATAGGATGTAAGTGAATGAAATGGTGAAG
Sp2-R	GATGTAAGTAGTTACGGAGCTCAC
tSp2-F	GAAATTAAATACGACTCACTATAGGG <u>CCCGG</u> ATAGCTCAGTCGGTAGAGCA <u>GCGGCCGG</u> ATGTAAGTGAATGAAATGGTG
tSp2-R	<u>CCCCAAGGGGTTATGCTATGGCGCCCGAACAGGGACTTGAACCCCTGGACC</u> <u>CGCGGCCGG</u> ATGTAAGTAGTTACGGAGCTC
p31b-F	CAGTCA <b>AGATCT</b> CGATCCCGCGAAATTAAATACGACTCACTATAGGG
p31b-R	CATCAG <b>CTCGAG</b> AAAAAAACCCCTCAAGACCCGTTAGAGGCCCAAGGG GTTATGCTA
yhjH-F	CATG <b>CATAT</b> GATAAGGCAGGTTATCCAGCG
yhjH-R	CATG <b>CTCGAG</b> TTATAGCGCCAGAACGCC
iLoy-F	GATC <b>CATATGGCGTCGTTCCAGTCGTC</b>
iLoy-R	GATC <b>GTCGAC</b> CTCGAGCAGCTTTCATATTCCCTCTGC
GFP-F	GATC <b>ATTAAT</b> TGCGTAAAGGAGAAGAACTTTCACT
GFP-R	CATG <b>CTCGAG</b> TCACTGGTGGTGGTGGTGGACTAAAGCGTAGTTT CGTC
dSens-F	TGCTTAAGTCGAACAGAAAGTAATCGTATTGTACACGGCCGCATAATCGAAAT
dSens-R	GGTTTCTTACCAAGACTCGACAAAAAAACCCCTCAAGACCC
dWspR-F	ctttaagaaggagatataccatgcacaaccctcatgagagcaagaccgacctggg
dWspR-R	cttctgttcacttaaggcatcagccccggggggccggcg
dYhjH-F	ctttaagaaggagatatacc <b>TATGATAAGGCAGGTTATCCAGCG</b>
dYhjH-R	cttctgttcacttaaggca <b>TTATAGCGCCAGAACCGCCG</b>

**Table S2 – Phylogenetic Sequences.**

Riboswitch sequences used in the phylogenetic analysis of GEMM-I riboswitch-Spinach fusions. Each sequence listed here was ordered as an ultramer flanked by the Sp sequences listed in **Table S3**.

Name	Sequence (5'→3')	Accession ID	Range
Aa-20	GCGTTTCAAGGGCAAACCAACGGAAACGTTGGGA CGCAAAGCTACGGGTCTACGGGGACTTGGACCT AAGACCGCCGGGCTGCCGC	ACCS0100001 .1	47422- 47506
Ac-480	TTTGAATGGTAAACCTGGTAAAAACCAGTGACA CAAAGCTACGGGTCTAAGGTCTTGACTAAGACA GCCGAGTTGCCGAA	AEDB01000061 .1	5163-5244
Al-1038	GATTAAAAGGCAAACCTAACGTAACCTAACGGACG CAAAACTAAAGGGCTAATTAGTAATAGACAGGCC AGTTGCATC	CP000896.1	1029331- 1029407
Am-205	ATGTAAGGCAAACCATGCAAACAAATGGGACG CAAAGCCAGGAACCTAAAGTGTGTTATAAAAAAA TATACCAAGATCGTCCGACTGCCAT	CP000724.1	3839671- 3839762
Bc-52	AAAATTGAAAAAGGCAAATTCATCGAAAGGTGGA GACGCAAAGCTAAAGGGACTAAAGTCAGATGAC CATGTCAGCCAGTTACCGATTT	CP003056.1	2189769- 2189858
Bc-58	CCTACCAGATAAAGGCAAATCTATTGAAAAGTAG AGGCGAAAACTACGGATCTAAGGGCTAAATGT TTAATGTCTATGATAGCCGGTTACCTAGTAGG	CP002394.1	854052- 854151
Bm-66	TGTACAGACAAGGGCAAACCAAGTTGAAAGGCTG GGACGCAAACCTCGGGCTAACGGTCACAGGAC TAGGACGGCCGGTTCTGATACA	CP003017.1	3889771- 3889861
Bs-46	TTAGAAAAGGCAAATCTGTGAAATCAGATGACG CAAAGCCACGGACCTAACGGTTCCCACGGTC GCCGGCTACCAAA	CP001791.1	2058948- 2059028
Bs-75	TTATAGAAGGCAAACTCATCTGAAAAGGGAGGA CGCAAAGCCACGGGCCTACATGCAAAATATTATT TGTATATTGGCAGCCGGTTACCTGTAG	ABCF01000033 .1	2270-2364
Cc-284	GATCGATCAGCAAACTAGCGAAAGCTAGTGAC GCAAAGCTACAGGGATTCCCCTTTAACAGGGGA TGTCAGCCAGCTGCAGGATT	ADLJ01000004. 1	176355- 176441
Cd-371	TGGTATCTGATTCAAGGGCAAAGTCGCCGAAAGG TGACGGCGCAAACACTAGAGGGGCTACAGCGATA ATACGCCAAGCCAGCCAGTTGCCGGATATCA	CP000860.1	1941826- 1941922
Cf-1A	CGACAAACGGCAAACCCGCCAAGGTGGGGA CGCAAAGCCACGGGCCACGAGGTAGCCGA GCTACCG	CP001964.1	2407234- 2407304
Cf-1B	GTCAGCGACAACGGCAAACCCGCCAAGGT GGGGACGCCAGGGCCCACGAGGTCA GCCGAGCTACCGAACGAC	CP001964.1	2407228- 2407309
Cf-6	GGTCAGACAAGGGCACACCCGTCGCGAGGC GGCCGCAAAGCCACGGGACCCACGCGGTCAGC CGGGCTGCCGACC	CP002666.1	2316134- 2316210
Ck-208	TTGATAATAGCACACTTATCGAAAGGTAGGGTCG	CP000673.1	2377707-

	CAAAGCTATGGGTCTTAAGAAAATTATTTTCTAT GATTGCCAGGTTGCCAA		2377792
Cm-1041	TTCCTTCCGATAAAAGGCAAACCAAGTCGCGAGG CTGGGACGCAAAGCCACC CGGT CAGCAAACGGG CTGACAGCGGGTTACCGAAGAAAGGAA	FP565575.1	196189-196281
Cp-234	CTTTAAAAAAATGGGCAAATTAGAGAAATCTAAT GACGCAAAGCTATAGGGACTAAGGTTATAACTA TGTCAGCCAGTTGCCAAAG	CP000246.1	1695612-1695699
Cp-287	CGATAATAGCAAACCTAGTGAAA ACTAGCGACG CAAAACTATAGGGTCTCCTTAGATATTCTAAGAT GATAGCCAGTTACCG	CP000885.1	1913589-1913671
Cp-865	AGTCATTGGCAAAC TGTTGAAAGGCCAGGAC GCAAAGCCTCCGGTCTAAAGACATGTCGCCAG GATAGCGGGTTGCCACAT	AC167560.3	117626-117710
Cs-225	CGACAAAGGGCAAAC TTGCCGAAAGGT AAGGAC GCAAAGCCGAGGGTCTAAAGT GCGAGAGCATT TGACAGTCTGGCTGCCG	CP002109.1	3402849-3402931
Ct-116	TATAAACCGATAAAGGCAAAC TGTTGAAACGCA GTGACGCAAAGCTACAGGGGCTAAGGTCCGCCA GGGCTATGCCAGCCAGCTACC GGTTTATG	AFCE01000088 .1	13-108
Ct-256	ATGAAACAGGGCAAAC ATCACCGAAAGGTGATGA CGCAAAGCCATGGGTCTACTGTTTAAACAATG TTTAAAGCTATGATGCCAGGCTGCCAT	CP002416.1	1366451-1366546
Da-534	CCTTGATAAGGGCAAAC CTGTCGAAAGGCAGGG ACGCAAAGCTACAGGTCTAAAGCATTGCTAAG ACAGCTGGGTTGCCGGGG	ACJM01000030 .1	1763-1847
Da-702	AGCCGAGAATCAAGCCAACCCGCCCTCAGGCCGG GACGGAAAGCCACGGGTCTTCAGACAGCCGG GTTGCCCTCGGTT	CP000112.1	841125-841200
Da-707	TCTCTCGATAAAGGCAAACCGGGAGTAATCCG GTGACGCAAAGCCACGGGTCTTGACAGGA TCGCCGGTTCCCGAAGAGG	AAEW0200000 1.1	1141863-1141931
Dg-430	TCTGAAAAGGCAAACCTGTTGAAAGACAGGGAC GCAAAGCCATGAGTCTAAGGTTTGAAAGGGCT ATGACAGTCAGGCTGCCGG	AGJQ01000018 .1	12829-12915
Dp-1045	TGTGACAAAGGCAAACCACTCGAGAGGGTGGGA CGCAAAGCCAAGGGACCTAACGAGGGACACATG TTCCAGGGTCAGCCTAGCCGCCACA	ACJG01018181 .1	935-1025
Dp-17	CTTCTCGACAAAGGCAAACCCCTCCGCAGGGGG GGACGCAAAGCCCACGGAACTCCGCTGCTCCG CTCTCTCTCAGGGCAGCACGGAAAGTTGCCCGG GCCACCGAAAGAAG	CP002539.1	69968-70079
Dt-697	TATCCAGCCAAACCCGCCGCAAGGCAGGGACG GAAAGCCACGGGCCCCCGGGATTAAAAGTCAT AGCATACGCCAGCCGGTTGCCGGATG	ACJN02000003 .1	250970-251064
Gc-1044	AATTGAATTATT CATCGTAAACTATTGAAGATA GTGACACAAAGCCAAGGGTCTAAGGTCCCTCCA AACGGGATTATGACAGTCCGGTTGCCACATT	ACYC0100019 1.1	495-593
Gm-790	TCGACAATACTAAACCATCCGCAGGGTGGGAC GGAAAGCCTACAGGTCTCTGAGACAGCCGG	CP000148.1	1079467-1079540

	GATGCCGA		
Gs-761	CTCCGAAAAGAGTAAACCCATCGCAAGGTGGGG ACACAAAGCCGACGGGTGCCGCTGGAGCGGGGA CGGCCGGGTTGCCGGAG	CP002031.1	2659688- 2659769
Hm-646	TGCTTATGGTAAACCCGTTGAAAGACGGGAC ACAAAGCCACCGACCTACAGCATCAATGCCATG GTAGCGGGGCCGCCA	ABRM0103182 9.1	2236-2316
Lb-336	TTTCATTGGCAAAGCCGGCGAAAGCCGGTGAC GCAAAGCTAGAGGGCCTGTATCCGTTATTCGG TATGTGGCAGCCAGTTGCCAAA	ACTP01000092 .1	157432- 157518
Mm- 662	GCATTTGAAAAAGGCAAACCTCAGCTGAAAAGCG AGGGCGCAAATCACCGGTCTAAGGGCGTAAG TTCTAAGATAGCGGGAGTACCAAGATGT	CP001672.1	134554- 134646
Oi-125	ATCCTCAGAAAAAGGCAAACCTATTGAAAGATGG GGACGCAAAGTCACAGATCTAAGGTATTTTACT AAGATGGCTGGACTATCTGGAT	BA000028.3	2580241- 2580330
Pc-822	ATTTTCGTTCAAGGCAAAGTCAGAGTAATCTGGC CACGCAAACACCACGGGTCCATGGTTCATGGATA GCCGGGTTGCCGAAAAT	CP000142.2	1774617- 1774700
Pi- 1049A	TATTGAAAAAGGCAAACCTCATCGAAAGGTGAGG GCGCAAAGCTACAGGAGCTAACCGATTCAATC GCCATGCTAGCCAGCTACCAAGTA	AATU01015137 .1	1224-1312
Pi- 1049B	TCCGTATTGAAAAAGGCAAACCTCATCGAAAGGTG AGGGCGCAAAGCTACAGGAGCTAACCGATTCA ATCGCCATGCTAGCCAGCTACCAAGTAAAGA	AATU01015137 .1	1220-1316
PI-156	CTACGATAACGGCAAACCTGTCGAAAGATAAGGA CGCAAAGCCACAGGGCCTTCTTGATGAACCGTC AATGGCAGCCTGGCTACCGAAG	AGIP01000013. 1	159170- 159258
Pm-140	CATTCTTTCATGGCAAACCTGCCGAAAGGCAG GGACGCAAAGCTTAGGGTCTACGGTCCTGCAGG GAATGACAGCCTGGCCGCCAATG	CP002869.1	30538- 30629
Pt-160	CGTTAACGCTAAACACCTCGAAAGTGGTGGACA CAAAGCCATGGGTCTAAAGCTGGATTAAACAGC CATGATTGCCAGGTTGCCG	CP003107.1	4365888- 4365972
Rc- 1047	CGAAGTAGTAACAAGGGCAAATCCATCGAAAGA TGGAGACGCAAATCACCGGTCTACGGGCTTAT GCCACGACAGCGGGATTGCCGGCTTCG	AASG0203014 3.1	245-337
Sd-919	CTGTGGAAGGCAAACCAGTTTAAAGACTGGGA CGCAAAGCCTCCGATCTAAAGGTTGCTTGTACC TATGATAGCGGGGATCCCACAG	CP000302.1	2534230- 2534318
Sp-917	CACTTGATGAAAAAGGCAAACCTGTGAAAGCA GGTGACGCAAAGCATCCAGCCTAACGGGACACC TATGGCAGTGGCGCTACCGCAAGTG	CP000851.1	4449054- 4449144
St-303	CCCCAGCGATAAAGGCACACCCGCCGAAAGACG GGGCCGCAAAGCCACGGGCTACAGGAAGCGG GCGCCGCCCTGCCGGTCTCCGCCTCCCATG CTAGCCGGGCTGCCGCTCGGG	AP006840.1	3227381- 3227498
Sv-921	TTTGAATAAAAGGCAAACCAATCGAAAGATTGGG ACGCAAAGCCTCCGGTCTAACGGGATAGTGTG AGGCAGGTCGTTGTCTCAGTATTATCGCAGTACCT	AP011177.1	990518- 990640

	AAGATAGCGGGGATACTTCAGG		
Ta-882	GCTCCCGAAACGGCAAACCTCCGGGTAAACCGGAT GTACGCAAAGCCACAGGTCTTTGAGTCATCAT CAGGACAGCTGAGCTACCGAAGGAGC	CP001616.1	1034200- 1034292
Td-659	ATCCCAGAAAGGGCAAACCCGCCGAGGGCGGG GGCGCAAAGCGACC GGCTCGAAAGAGATAGC GGCGCTGCCGTGGAT	CP000116.1	532900- 532978
To-592	TTCCGTCAAGGGCAAACCGTCGAAAGGTAGGGA CGCAAAGCCACGGGCCTACGAAGAGACAAGCTC TTCATAGCAGCCGGGCTGCCGGGG	CP002131.1	1785218- 1785307
Tt-888	CTCTGATAAAAAGGCACGCTGACGCGAAAGCCC AGCACGCAAATTACCGGTCTAAGGACTCAAGG TCTACGACAGCGGGATGCCAGAG	CP001614.2	634814- 634903
Vn- 1026	GCTCAAAAGGCAAAC TTGCTTAAAGCAGGGAC GCAAAATGACAGTGCCACTGATTTGGAGAGG ATTATTGGCAGGCTGCATTACAAGAGC	AFWJ01000289 .1	14511- 14603

**Table S3 – Flanking Sequences.**

All riboswitch-Spinach fusions were flanked by the following Spinach or Spinach2 sequences on their 5' and 3' sides.

Sp 5'	GACGCGACTGAATGAAATGGTGAAGGACGGGTCCA
Sp 3'	TTGTTGAGTAGAGTGTGAGCTCCGTAAGTAGTCGCGTC
Sp2 5'	GATGTAACTGAATGAAATGGTGAAGGACGGGTCCA
Sp2 3'	TTGTTGAGTAGAGTGTGAGCTCCGTAAGTTACATC